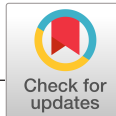




Title	Ubiquitin carboxyl-terminal hydrolase L1 promotes hypoxia-inducible factor 1-dependent tumor cell malignancy in spheroid models
Author(s)	Li, Xuebing; Hattori, Akira; Takahashi, Senye; Goto, Yoko; Harada, Hiroshi; Kakeya, Hideaki
Citation	Cancer science (2020), 111(1): 239-252
Issue Date	2020-01
URL	<a href="http://hdl.handle.net/2433/251040">http://hdl.handle.net/2433/251040</a>
Right	© 2019 The Authors. Cancer Science published by John Wiley & Sons Australia, Ltd on behalf of Japanese Cancer Association. This is an open access article under the terms of the Creative Commons Attribution NonCommercial License, which permits use, distribution and reproduction in any medium, provided the original work is properly cited and is not used for commercial purposes.
Type	Journal Article
Textversion	publisher



# Ubiquitin carboxyl-terminal hydrolase L1 promotes hypoxia-inducible factor 1-dependent tumor cell malignancy in spheroid models

Xuebing Li<sup>1</sup> | Akira Hattori<sup>1</sup> | Senye Takahashi<sup>1</sup> | Yoko Goto<sup>2</sup> | Hiroshi Harada<sup>3</sup>  | Hideaki Takeya<sup>1</sup> 

<sup>1</sup>Division of Bioinformatics and Chemical Genomics, Department of System Chemotherapy and Molecular Sciences, Graduate School of Pharmaceutical Sciences, Kyoto University, Kyoto, Japan

<sup>2</sup>Department of Radiation Oncology and Image-applied Therapy, Graduate School of Medicine, Kyoto University, Kyoto, Japan

<sup>3</sup>Laboratory of Cancer Cell Biology, Graduate School of Biostudies, Kyoto University, Kyoto, Japan

## Correspondence

Hideaki Takeya, Division of Bioinformatics and Chemical Genomics, Department of System Chemotherapy and Molecular Sciences, Graduate School of Pharmaceutical Sciences, Kyoto University, 46-29 Shimoadachi-cho, Yoshida, Sakyo-ku, Kyoto 606-8501, Japan.  
Email: scseigyohisyo@pharm.kyoto-u.ac.jp

## Funding information

A Grant-in Aid for Scientific Research on Innovative Areas "Frontier Research on Chemical Communications" from Ministry of Education, Culture, Sports, Science and Technology (MEXT), Japan, Grant/Award Number: No. 17H06401; A Grant-in-Aid for Scientific Research from Ministry of Education, Culture, Sports, Science and Technology (MEXT), Japan, Grant/Award Number: No. 19H02840; The Project for Development of Innovative Research on Cancer Therapeutics (P-DIRECT) from Japan Agency for Medical Research and Development (AMED), Japan, Grant/Award Number: No. 15cm0106117h0002; The Platform Project for Supporting Drug Discovery and Life Science Research from Japan Agency for Medical Research and Development (AMED), Japan, Grant/Award Number: No. JP19am0101092

## Abstract

Hypoxia-inducible factor 1 (HIF-1) is a critical heterodimeric transcription factor for tumor malignancy. Recently, ubiquitin carboxyl-terminal hydrolase L1 (UCHL1) has been reported to function as a deubiquitinating enzyme for the stabilization of its  $\alpha$  subunit (HIF-1 $\alpha$ ). In the present study, we showed that UCHL1 inhibition can be an effective therapeutic strategy against HIF-1-dependent tumor malignancy. In 2D monolayer culture, a UCHL1 inhibitor suppressed HIF activity and decreased the transcription of HIF downstream genes by inhibiting the UCHL1-mediated accumulation of HIF-1 $\alpha$ . Phenotypically, UCHL1 inhibition remarkably blocked cell migration. In 3D spheroid culture models, ectopic expression of UCHL1 significantly upregulated malignancy-related factors such as solidity, volume, as well as viable cell number in an HIF-1 $\alpha$ -dependent manner. Conversely, inhibition of the UCHL1-HIF-1 pathway downregulated these malignancy-related factors and also abolished UCHL1-mediated cell proliferation and invasiveness. Finally, inhibition of UCHL1 promoted HIF-1 $\alpha$  degradation and lowered the expression of HIF-1 target genes in the 3D model, as also observed in 2D monolayer culture. Our research indicates that the UCHL1-HIF-1 pathway plays a crucial role in tumor malignancy, making it a promising therapeutic target for cancer chemotherapy.

## KEYWORDS

hypoxia-inducible factor 1, molecular target, spheroid, tumor malignancy, ubiquitin carboxyl-terminal hydrolase L1

This is an open access article under the terms of the Creative Commons Attribution-NonCommercial License, which permits use, distribution and reproduction in any medium, provided the original work is properly cited and is not used for commercial purposes.

© 2019 The Authors. *Cancer Science* published by John Wiley & Sons Australia, Ltd on behalf of Japanese Cancer Association.

## 1 | INTRODUCTION

Ubiquitin carboxyl-terminal hydrolase L1 (UCHL1) is a 223-amino acid protein that belongs to the ubiquitin carboxyl-terminal hydrolase (UCH) family of deubiquitinating enzymes.<sup>1,2</sup> UCHL1 catalyzes the release of a ubiquitin (Ub) moiety from C-terminal extended Ub, such as Ub precursors and C-terminal Ub thioesters, to generate a monomeric Ub pool via de novo synthesis and salvage pathways.<sup>3</sup> It is also reported that UCHL1 digests poly-Ub chains conjugated to  $\beta$ -catenin by SCF <sup>$\beta$ -Trcp</sup> E3 ligase complex.<sup>4,5</sup> Conversely, homodimeric and membrane-associated farnesylated UCHL1 is able to catalyze the formation of Lys48-linked poly-Ub chains on  $\alpha$ -synuclein by acting as an E3 Ub ligase.<sup>6</sup>

Ubiquitin carboxyl-terminal hydrolase L1 was originally identified as a brain-specific protein, known as protein-gene-product (PGP) 9.5, by 2D polyacrylamide gel electrophoresis analysis.<sup>7</sup> The distribution of this enzyme in normal tissue is known to be highly limited, particularly in the brain,<sup>8</sup> and moderately expressed in the pancreas,<sup>9</sup> testis<sup>10</sup> and urinary bladder.<sup>11</sup> Aberrant expression of UCHL1 has been reported in renal cancer,<sup>12</sup> non-small cell lung cancer,<sup>13</sup> gastric cancer<sup>14</sup> and colorectal cancer.<sup>5</sup> In colorectal tumor tissues, UCHL1 was shown to activate the  $\beta$ -catenin/TCF signaling pathway by releasing an Ub moiety conjugated to  $\beta$ -catenin, resulting in the promotion of tumor malignancy.<sup>15</sup>

Hypoxia-inducible factor (HIF) is known to have pivotal roles in tumor malignancy<sup>16</sup> and is considered a promising molecular target for cancer chemotherapy.<sup>17-19</sup> HIF is a heterodimeric protein comprising  $\alpha$  and  $\beta$  subunits: HIF-1 $\alpha$ , HIF-2 $\alpha$  and HIF-3 $\alpha$ , and HIF-1 $\beta$ .<sup>20,21</sup> The protein expression levels of HIF-1 $\alpha$  and HIF-2 $\alpha$  are oxygen-dependent and are tightly regulated by the ubiquitin-proteasome pathway.<sup>22</sup> Briefly, under aerobic conditions, two proline residues in the oxygen-dependent degradation (ODD) domain (eg, Pro-402 and Pro-564 of human HIF-1 $\alpha$ ) are hydroxylated by a dioxygenase named prolyl-4-hydroxylase (PHD).<sup>23</sup> The von-Hippel-Lindau tumor suppressor-elongin B/C-cullin 2 (VHL-EloBC-Cul2) E3 ligase complex is recruited onto the hydroxylated Pro-residues, and conjugates Lys48-linked poly-Ub chain on the  $\epsilon$ -NH<sub>2</sub> residue of HIF-1 $\alpha$  and HIF-2 $\alpha$ .<sup>24</sup> Conversely, in hypoxic microenvironments such as those in solid tumors,  $\alpha$  subunit escapes degradation and is translocated to the nucleus, forming a heterodimer with HIF-1 $\beta$ .<sup>25</sup> HIF specifically transactivates a variety of genes under promoter containing hypoxia-responsive elements (HRE), including *GLUT1* and *CA9*.<sup>20,26</sup> Previously, we reported that UCHL1 functions as a deubiquitinating enzyme for the stabilization of HIF-1 $\alpha$  while blockade of the UCHL1-HIF-1 $\alpha$  pathway suppresses the formation of metastatic tumors in mouse models.<sup>27</sup>

Recently, 3D culture systems have been increasingly and widely applied in preclinical studies to provide more physiologically relevant information. Compared with 2D cell culture, 3D cultured cells exhibit more similarities with tumor tissues with regards to cell morphology, proliferation, stage of cell cycle, gene expression and drug sensitivity.<sup>28</sup> Among these, higher expression of HIF-1 $\alpha$  is considered as a critical factor that contributes to these features of 3D culture.<sup>29</sup>

Therefore, we consider it crucial to elucidate the significance of the UCHL1-HIF-1 $\alpha$  pathway in a 3D culture system.

In the present study, we investigated the potential roles of UCHL1 in cancer therapeutic approaches using a 3D spheroid culture system. We revealed that depletion of *UCHL1* by siRNA or blockade of its deubiquitinating activity with a specific inhibitor caused a remarkable decrease in HIF-1 $\alpha$  protein levels in 3D spheroid culture models. Resulting reduction in expression of HIF-1 $\alpha$  target genes in the spheroids, which are closely related to tumor malignancy including metastasis, cell proliferation and angiogenesis, was observed. These findings suggest that the UCHL1-HIF-1 $\alpha$  pathway is a promising therapeutic target in anticancer chemotherapy.

## 2 | MATERIALS AND METHODS

### 2.1 | Plasmids and purification of recombinant protein

To construct pGEX6p-2/UCHL1, DNA encoding human *UCHL1* gene was digested between *EcoRV* and *XhoI* in pcDNA4/UCHL1. This DNA fragment was then inserted between the *SmaI* and *XhoI* sites of pGEX6p-2 (Invitrogen). *E coli* DH5 $\alpha$  harboring pGEX6p-2/UCHL1 plasmid was induced with isopropyl  $\beta$ -D-1-thiogalactopyranoside. *E coli* DH5 $\alpha$  was treated with sonication and dissolved in lysis buffer (50 mmol/L Tris-HCl [pH 8.0], 0.1 mol/L NaCl, 1 mmol/L EDTA, 1 mmol/L DTT, 1% Triton X-100) The fusion protein GST/UCHL1 was first purified with glutathione-Sepharose 4B beads (GE Healthcare UK) and eluted with 20 mmol/L of glutathione (GSH; pH 8.5).

### 2.2 | Cell culture and reagents

HeLa, MDA-MB-231 and MDA-MB-436 cells were purchased from the American Type Culture Collection. Cells were incubated in DMEM containing 10% FBS and cultured in a well-humidified incubator with 5% CO<sub>2</sub> and 95% air. For <0.1% O<sub>2</sub> hypoxic incubation, cells were kept in a Bactron Anaerobic Chamber, BACTRONEZ (Sheldon Manufacturing, Cornelius). For <1% O<sub>2</sub> incubation, cells were kept in a multi-gas incubator, MCO-5M (Panasonic). Camptothecin (CPT) and LDN57444 were obtained from FUJIFILM Wako Pure Chemical and Sigma-Aldrich, respectively. For 2D culture, Falcon tissue culture plates from Corning are used.

### 2.3 | Transient transfection

In HeLa cells, Lipofectamine 2000 (Thermo Fisher Scientific) was used at a ratio of 3:1 (reagent : DNA) to transiently transfect HeLa/5HRE-Luc cells with pcDNA4/UCHL1 plasmid. In MDA-MB-231 and MDA-MB-436 cells, Lipofectamine LTX Reagent (Thermo Fisher Scientific) was used at a ratio of 9:1 (reagent : DNA) for transfection. Lipofectamine 3000 (Thermo Fisher

Scientific) was used at a ratio of 2:1 (reagent : DNA) and 1:10 ( $\mu\text{L}$  of reagent : pmol of siRNA) for the co-transfection in MDA-MB-231 cells.

## 2.4 | Luciferase assay and western blotting

For luciferase assays, HeLa/5HRE-Luc or HeLa/ ODD-Luc cells were seeded in 96-well plates at a concentration of  $1 \times 10^5$  cells/mL and incubated under normoxic conditions. After a 24-hour incubation, cells were treated with each reagent for 1 hour. Cells were then transferred to normoxic or hypoxic conditions for another 24-hour incubation and harvested in 100  $\mu\text{L}$  of passive lysis buffer (Promega). Luciferase assays were performed using 100  $\mu\text{L}$  of luciferase assay reagent (Promega) or dual luciferase assay kit (Promega) according to the manufacturer's instructions. Western blotting analysis was performed using anti-HIF-1 $\alpha$  (BD Biosciences), anti-UCHL1 (R&D Systems), anti- $\alpha$ -tubulin (Sigma-Aldrich), anti- $\beta$ -actin (Sigma-Aldrich) and anti- $\beta$ -tubulin (Abcam) as primary antibodies. Alkaline-phosphatase conjugated goat anti-mouse IgG antibody (Promega) was used as the secondary antibody. 5-Bromo-4-chloro-3-indolyl-phosphate 4-toluidine salt (BCIP) and nitroblue tetrazolium (NBT) (Nacalai Tesque) was used to detect the indicated proteins.

## 2.5 | Wound healing assay and transwell migration assay

In the wound healing assay, MDA-MB-231 and MDA-MB-436 cells were seeded at a concentration of  $5 \times 10^5$  cells/mL into 24-well plates (Corning). A wound was stimulated perpendicularly in each well of cells by scratching the cells with 200- $\mu\text{L}$  pipette tips. Cells were washed with PBS (-) to remove debris and then incubated under normoxia or hypoxia. After 8, 24 and 48 hours, the recovery of gaps was measured by microscopy. In the transwell migration assay, MDA-MB-231 and MDA-MB-436 cells were seeded at a concentration of  $5 \times 10^5$  cells/mL in Chemotaxicell chambers (8.0  $\mu\text{m}$  pore; Kurabo) inserted into 24-well plates (Corning). Cells were pre-incubated with DMEM containing 10% FBS for 24 hours and transferred into serum-free medium with chemoattractant for another 24-hour incubation period. Cells were immobilized with methanol and stained with crystal violet (Nacalai Tesque). The number of migrated cells was counted under the microscope.

## 2.6 | siRNA transfection

For the depletion of UCHL1 and HIF-1 $\alpha$  in MDA-MB-436 cells, cells were plated in 6-well or 24-well tissue culture plates (Corning) at a concentration of  $1.2 \times 10^5$  cells/mL and cultured in antibiotic-free DMEM medium containing 10% of FBS. For transfection of 6-well or 24-well cultures, 10 or 50 pmol of siRNA

(siUCHL1: silencer Select Validated siRNA, Cat# 4390824-s14616; Thermo Fisher Scientific: 5'-AAGUUAGUCCUAAAGUGUATT-3', 4390824-s14617: 5'-GCACAAUCGGACUUAUUCATT-3' siHIF-1 $\alpha$ : silencer Select Validated siRNA, Cat# 4390824-s6539 and Cat# 4390824-s6541) with Lipofectamine RNAiMAX or Lipofectamine 3000 (Thermo Fisher Scientific) was used, respectively. After 48-hour transfection, the cells were lysed and subjected to western blotting analysis or immunofluorescent staining. For the negative control, scrambled siRNA (Cat# 12935-300, sequence information not disclosed; Life Technologies) was used. For 3D culture, cells were first cultured and transfected with siRNA as indicated above, then collected after a 24-hour incubation and cultured on 3D culture 96-well plates (Corning).

## 2.7 | Immunofluorescent staining

For HIF-1 $\alpha$  and UCHL1 staining in 2D culture, cells treated with each condition were washed with PBS (-) and fixed in 4% paraformaldehyde at room temperature for 15 minutes, followed by permeabilization with 0.1% Triton X-100 for 10 minutes on ice. The coverslips were blocked with 3% BSA for 12 hours and incubated with anti-HIF-1 $\alpha$  (1:500; BD Biosciences) and anti-UCHL1 (1:500; R&D Systems) antibodies for 1 hour at 4°C. After three 5-minute washes with PBS (-), samples were probed with goat anti-rabbit polyclonal secondary antibody (Alexa Fluor 488, 1:1000; Abcam) or goat anti-mouse polyclonal secondary antibody (Alexa Fluor 568, 1:1000; Abcam) mixed with 4',6-diamino-2-phenylindole (DAPI) (1:5000, Roche) at room temperature for 1 hour. The coverslips were mounted onto slides with Dako Fluorescence Mounting Medium (Agilent). Fluorescence was detected by fluorescence microscopy (Olympus).

## 2.8 | Quantitative RT-PCR analysis

For 2D culture, total RNA was extracted from cells untreated or treated with 3.7  $\mu\text{mol/L}$  LDN57444 for 24 hours using the Total RNA Extraction Miniprep System (Viogene). Reverse transcription was performed using ReverTra Ace qPCR RT Master Mix with gDNA Remover (TOYOBO). Quantitative real-time PCR (qRT-PCR) reactions were performed in duplicate in a 20- $\mu\text{L}$  volume containing 0.25  $\mu\text{mol/L}$  of each primer, 2  $\mu\text{L}$  of cDNA template and  $1 \times$  SYBR Green (Applied Biosystems). qRT-PCR was performed using the StepOnePlus Real-Time PCR System (Thermo Fisher Scientific) according to the manufacturer's instructions. The primers used for PCR were as follows: human *GLUT1*: 5'-TGACAAGACACCCGAGGAGC-3' (forward), 5'-GTCCAGCCCTACAGATTAGC-3' (reverse); human *CA9*: 5'-AACGTCCCACCTGCTGCTTTT-3' (forward), 5'-TGTACAGCTTCAGTTTCCCCCGGA-3' (reverse); and human *HIF1 $\alpha$* : 5'-TACTAGCTTTCAGAATGCTC-3' (forward), 5'-GCCTGTATAGGAGCATTAAAC-3' (reverse). The relative expression levels of *HIF1 $\alpha$* , *GLUT1* and *CA9* mRNA were normalized to 18S RNA.

## 2.9 | 3D culture and cell viability analysis

In the 3D culture, cells were cultured at a concentration of  $1 \times 10^5$  cells/mL on ultra-low attachment (ULA) spheroid microplates (Corning) for specific time periods. The viability of cultured cells was measured using the CellTiter-Glo Luminescent Cell Viability Assay (Promega).

## 2.10 | Morphological analysis of 3D tumor cultures

To evaluate characteristics including equivalent diameter, spheroid area, volume, solidity and sphericity, images of spheroid cells were taken using an Olympus CKX53 inverted microscope. Photos were

then processed with open source image processing suites written in MATLAB (The MathWorks), AnaSP and ReViSP to acquire 3D brightfield images and morphological 2D and 3D malignancy-related factors.

## 2.11 | Spheroid invasion assay

Five days after plating in ULA spheroid microplates, the culture medium was changed to DMEM, containing FBS (final concentration = 10%), penicillin-streptomycin (final concentration = 1%), collagen I (final concentration = 0.5 mg/mL) and basement membrane extract (BME; final concentration = 5 mg/mL). Photo of cells was

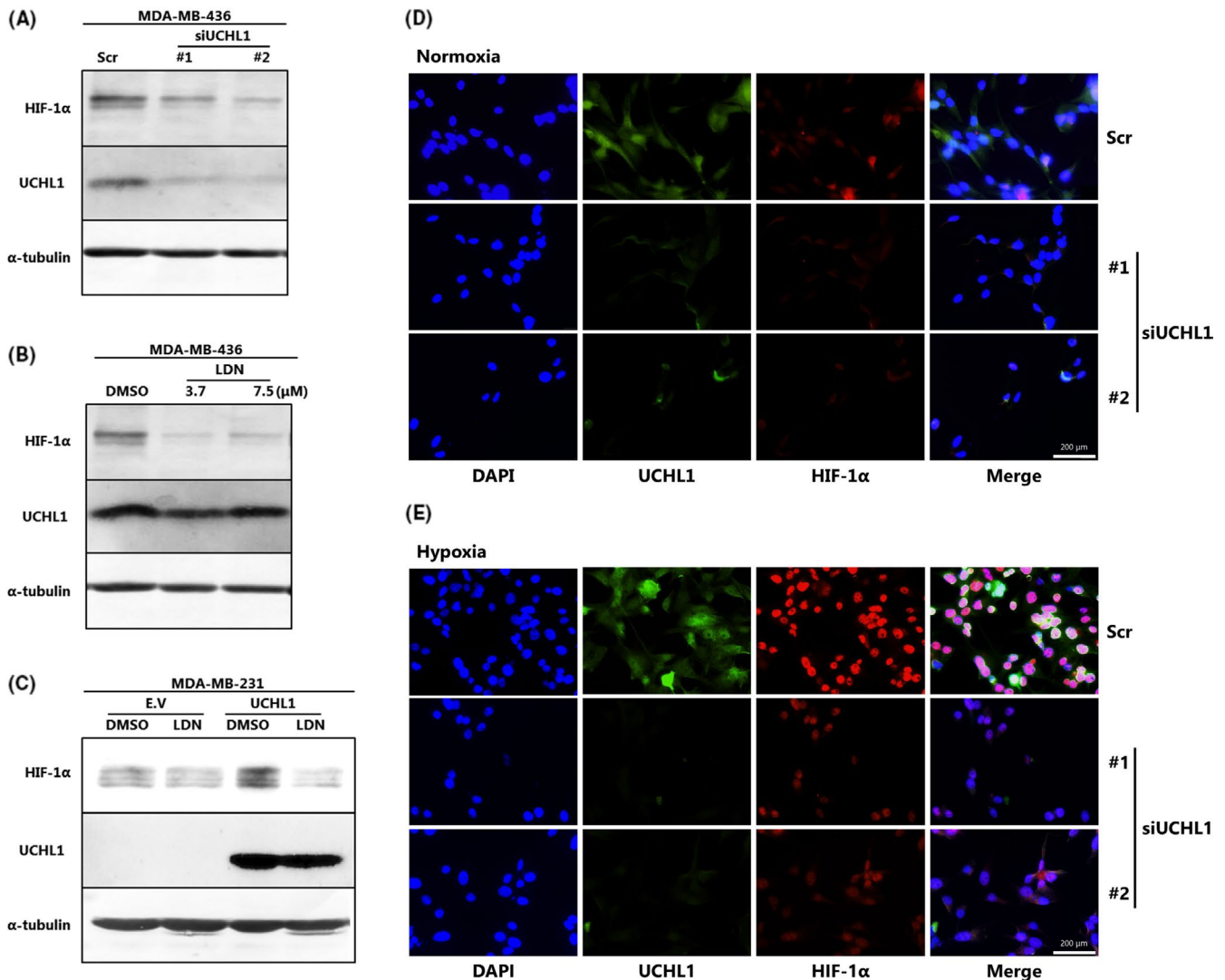


**FIGURE 1** Ubiquitin carboxyl-terminal hydrolase 1 (UCHL1) is involved in the regulation of hypoxia-inducible factor 1α (HIF-1α) protein expression. A, Scrambled siRNA (Scr) or UCHL1-siRNA (siUCHL1) transfected MDA-MB-436 cells were incubated under hypoxic conditions (1%  $O_2$ ) for 24 h before western blotting analysis using the indicated antibodies. B, MDA-MB-436 cells were treated with 3.7 or 7.5 μmol/L of LDN57444 under normoxia (21%  $O_2$ ) for 24 h and then incubated under hypoxia (1%  $O_2$ ) for another 24 h. Cells were then lysed and subjected to western blotting analysis. C, MDA-MB-231 cells were transiently transfected with either pcDNA4/UCHL1 (UCHL1) or pcDNA4/myc-His A (empty vector (EV)) and treated with DMSO or LDN57444 (3.7 μmol/L) under normoxia (21%  $O_2$ ) for 24 h. Cells were then transferred to hypoxia (1%  $O_2$ ) for another 24 h incubation before western blotting analysis. D, E, Scr- or siUCHL1-transfected MDA-MB-436 cells were incubated under hypoxic conditions (1%  $O_2$ ) for 24 h. Cells were then fixed and subjected to immunostaining

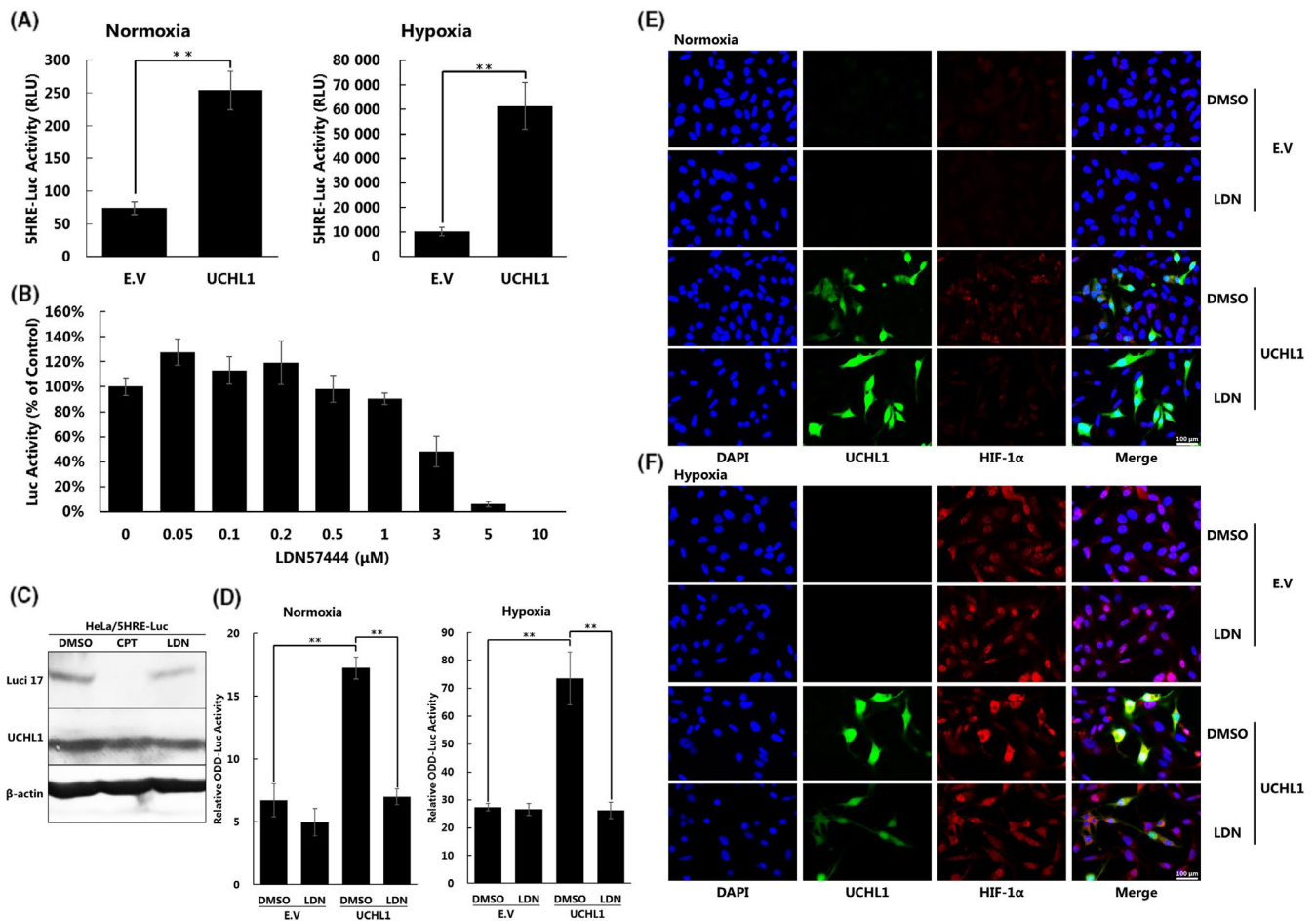


**FIGURE 2** Ubiquitin carboxyl-terminal hydrolase L1 (UCHL1) inhibition or deficiency lowers hypoxia-inducible factor (HIF-1) activity and blocks the metastatic potential of tumor cells. A, HeLa/5HRE-luciferase cells were transiently transfected with either empty vector (EV) or UCHL1. Cells were then transferred to normoxic (21% O<sub>2</sub>) or hypoxic (1% O<sub>2</sub>) conditions for 5HRE-luciferase assays. B, 5HRE-luciferase-UCHL1 cells were treated with various concentrations of LDN57444 for 1 h and transferred to hypoxic conditions for another 24 h incubation before measuring luciferase activity. C, 5HRE-luciferase-UCHL1 cells were treated with DMSO, camptothecin (CPT; 0.25 μmol/L) or LDN57444 (3.7 μmol/L) for 1 h and incubated under hypoxic conditions for 24 h to be subjected to western blotting analysis. D, HeLa/ODD-Luc cells were treated with LDN57444 (3.7 μmol/L) or DMSO for 1 h under normoxia and transferred to hypoxia for another 24-h incubation before obtaining luminescence measurements. Relative firefly luciferase activity was normalized using Renilla luciferase activity. E, F, MDA-MB-231 cells were transfected with the indicated plasmids and treated with LDN57444 (3.7 μmol/L) for 1 h under normoxia before being transferred to hypoxic conditions for a 4-h incubation. Immunostaining was then performed with the indicated antibodies. G, H, MDA-MB-231 or MDA-MB-436 cells were treated with LDN57444 (3.7 μmol/L) and maintained under normoxic or hypoxic conditions for another 24 h. RNA was then collected and subjected to RT-qPCR to quantify the mRNA levels of the indicated genes. I, J, Wound healing assays were conducted with MDA-MB-231 and MDA-MB-436 cells. Cells were treated with DMSO or LDN57444 (2.5 μmol/L) for 24 h and then scratched with a P200 tip. Recovery rate of scratched gaps were measured over time (middle) and after 48 h (right). K, L, Transwell migration assays were conducted with MDA-MB-231 and MDA-MB-436 cells. Cells were pre-incubated with serum-free medium for 24 h and transferred into 10% FBS/DMEM medium with DMSO or LDN57444 (2.5 μmol/L) for 24 h before measuring the number of migrated cells. M, MDA-MB-231 and MDA-MB-436 cells were treated with LDN57444 (2.5 μmol/L) and cell number was measured after 8, 24 and 48 h. Data is shown as mean ± SD; n = 3. Error bar indicates SD of the mean of three independent tests. \**P* < 0.05, \*\**P* < 0.01 was verified with Tukey's honestly significant difference test or Student's *t*-test

taken after another 2-day incubation. The surface area of the invaded cells was measured using ImageJ.<sup>30</sup>

## 2.12 | Spheroid viability staining and spheroid immunofluorescent staining

Five days after plating in ULA spheroid microplates, cells were stained with a mixture of 1 mmol/L of Calcein-AM, 1 mmol/L of

EthD-1 and 20 μmol/L of Hoechst 33342 for 4 hours and then imaged. Images were acquired with a confocal fluorescence microscope (Nikon) at room temperature. For 3D staining, spheroids were washed with PBS (-) and fixed in 4% paraformaldehyde at room temperature for 20 minutes and then permeabilized with 0.3% Triton X-100/PBS (-) and protease inhibitors for 20 minutes on ice. Samples were blocked with 3% of BSA/1% Triton X-100/PBS (-) at room temperature for 1 hour and incubated at 4°C with primary antibodies against HIF-1α (1:400; BD Biosciences) and anti-UCHL1 (1:400; R&D

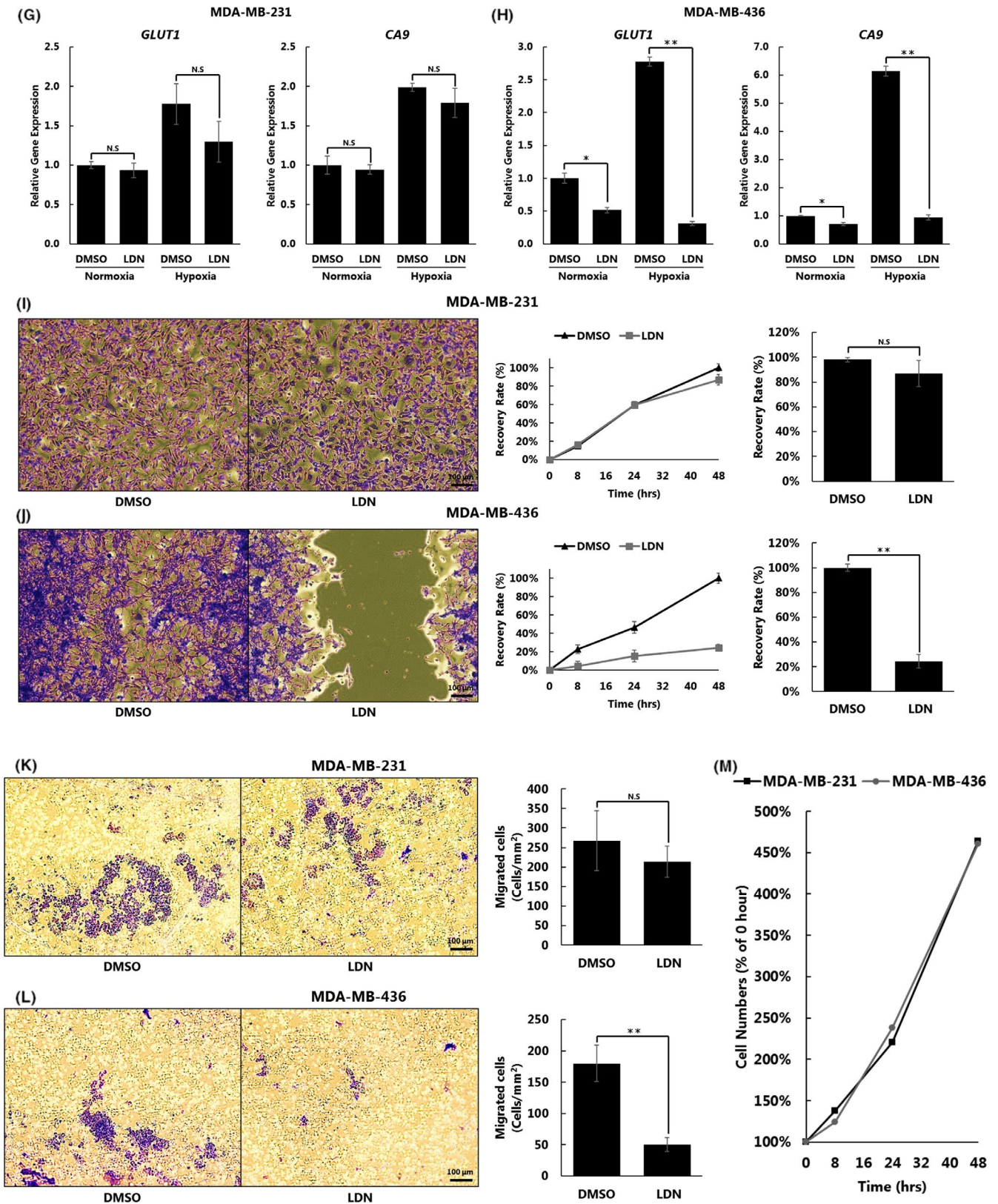
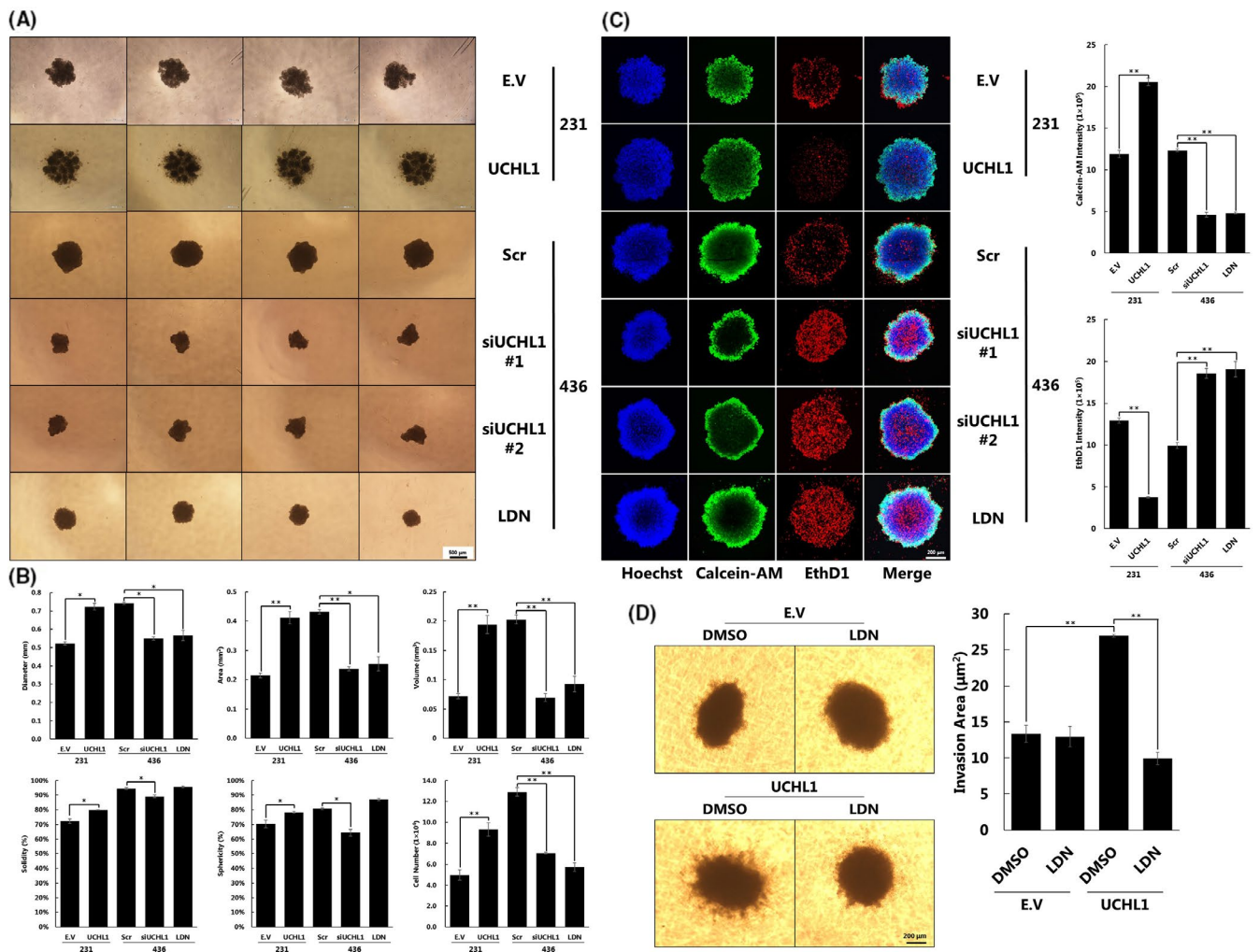


FIGURE 2 (Continued)

Systems) overnight. After three washes with 0.1% Triton X-100/PBS (-), samples were probed with goat anti-rabbit polyclonal secondary antibody (Alexa Fluor 488, 1:500; Abcam) or goat anti-mouse

polyclonal secondary antibody (Alexa Fluor 568, 1:500; Abcam) mixed with DAPI (Roche) at room temperature for 1 hour. Images were acquired with a confocal fluorescence microscope (Nikon) at



**FIGURE 3** Ubiquitin carboxyl-terminal hydrolase L1 (UCHL1) deficiency or inhibition leads to UCHL1-dependent cell death in 3D culture. A, MDA-MB-231 cells were transiently transfected with either empty vector (EV) or UCHL1. MDA-MB-436 cells were transfected with either scrambled siRNA (Scr), or UCHL1-siRNA (siUCHL1), or treated with LDN57444 (15 μmol/L). Cells were seeded on ultra-low attachment (ULA) spheroid microplates and incubated for 6 d before imaging. B, Corresponding 3D reconstructions of cells were obtained using ReVISP. Malignancy-related factors including equivalent diameter, spheroid area, volume, solidity and sphericity were further analyzed with AnaSP. Spheroid cell number was measured with a CellTiter-Glo 3D cell viability assay. C, UCHL1- or mock-transfected MDA-MB-231 cells, and siUCHL1-transfected or Scr-transfected or LDN57444 (15 μmol/L)-treated MDA-MB-436 cells were seeded on ULA spheroid microplates. On the last day of incubation, cells were stained with Hoechst 33342 (blue), Calcein-AM (green) and EthD1 (red) for imaging by confocal fluorescence microscopy. D, UCHL1-transfected or mock-transfected MDA-MB-231 cells were seeded on ULA spheroid microplates for 6 d. Medium was replaced with a mixture of DMEM, FBS, Collagen I, basement membrane extract (BME), and DMSO or LDN57444 (15 μmol/L) for another 2-d incubation period. The surface area of the invaded cells was measured using ImageJ. Data is shown as mean ± SD; n = 3. Error bar indicates SD of the mean of three independent tests. \**P* < 0.05, \*\**P* < 0.01 was verified with Tukey's honestly significant difference test or Student's *t*-test

room temperature. Fluorescent intensity was quantified using cellSens software (Olympus).

### 3 | RESULTS

#### 3.1 | Ubiquitin carboxyl-terminal hydrolase L1 is involved in the regulation of hypoxia-inducible factor 1α protein expression

Because UCHL1 has been reported to stabilize HIF-1α with its deubiquitinating activity, we first tested whether knockdown of *UCHL1* gene

could lead to a decrease in the protein levels of HIF-1α. As expected, less HIF-1α accumulation was confirmed in human breast adenocarcinoma-derived MDA-MB-436 cells, which have endogenous UCHL1 expression, when treated with siUCHL1 compared with the mock group under hypoxia (Figure 1A). Under normoxia, due to the oxygen-dependent degradation, the HIF-1α immunoblotting signal was too weak to detect (data not shown). We further tested whether a UCHL1 inhibitor could have the same effect. We found that the well-known UCHL1 inhibitor, LDN57444 with an IC<sub>50</sub> of 3.7 μmol/L, lowered HIF-1α protein stability to the same extent as that of siUCHL1 (Figure 1B). We also examined whether the UCHL1 inhibitor could have the same inhibitory effect on HIF-1α accumulation in the case of ectopic UCHL1 expression. In



**FIGURE 4** Ubiquitin carboxyl-terminal hydrolase L1 (UCHL1) inhibition decreases viable cell number and invasiveness under 3D culture in a hypoxia-inducible factor 1 $\alpha$  (HIF-1 $\alpha$ )-dependent manner. A, MDA-MB-231 cells co-transfected with empty vector (EV)/UCHL1 and Scr/HIF-1 $\alpha$  siRNA (siHIF-1 $\alpha$ ) for 48 h and were collected to be applied to western blotting analysis. B, MDA-MB-231 cells co-transfected with EV/UCHL1 and Scr/siHIF-1 $\alpha$  were cultured in ULA spheroid microplates for 3 d to form spheroids. Medium was then replaced with a mixture of DMEM, FBS, collagen I, basement membrane extract (BME) and DMSO or LDN57444 (15  $\mu$ mol/L) for another 2-d incubation period. Quantification data for malignancy-related factors are shown in Figure S4. C, D, MDA-MB-231 cells co-transfected with EV/UCHL1 and scrambled/siHIF-1 $\alpha$  for 24 h and were collected to be cultured in ULA spheroid microplates for another 5 d before their images were taken (C) or spheroid viability staining was performed (D). Data is shown as mean  $\pm$  SD;  $n = 3$ . Error bar indicates SD of the mean of three independent tests. \* $P < 0.05$ , \*\* $P < 0.01$  was verified with Tukey's honestly significant difference test or Student's  $t$ -test

MDA-MB-231 cells, a human breast cancer cell line with no endogenous UCHL1 protein expression, protein expression of HIF-1 $\alpha$  was elevated by the overexpression of UCHL1, while LDN57444 treatment canceled this effect (Figure 1C). Because the translocation of HIF-1 $\alpha$  into the nucleus is necessary for its transactivation activity, we examined where silencing of *UCHL1* would affect HIF-1 $\alpha$  protein expression. Depletion of *UCHL1* lowered HIF-1 $\alpha$  protein expression not only in the nucleus but also in cytosol under both normoxia and hypoxia, indicating that the stabilization of HIF-1 $\alpha$  by UCHL1 is before its translocation into the nucleus (Figure 1D,E and S1). Taken together, UCHL1 was demonstrated to upregulate HIF-1 $\alpha$  protein expression, and its knockdown or pharmacological inhibition could counteract this effect.

### 3.2 | Ubiquitin carboxyl-terminal hydrolase L1 inhibition or deficiency lowers hypoxia-inducible factor 1 activity and blocks the metastatic potential of tumor cells

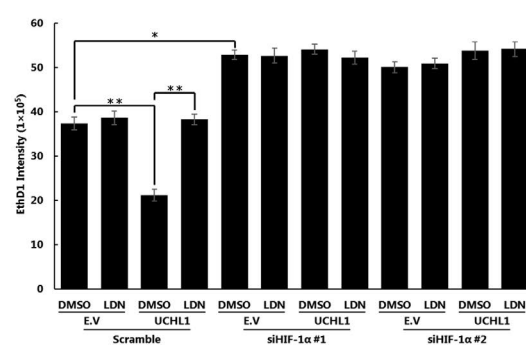
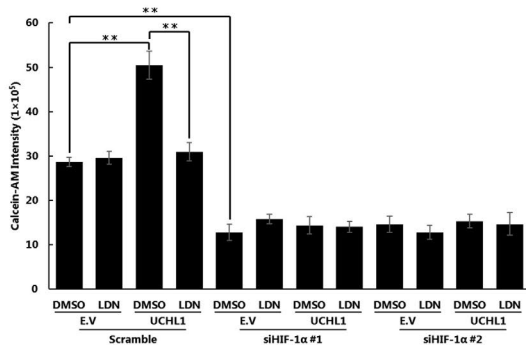
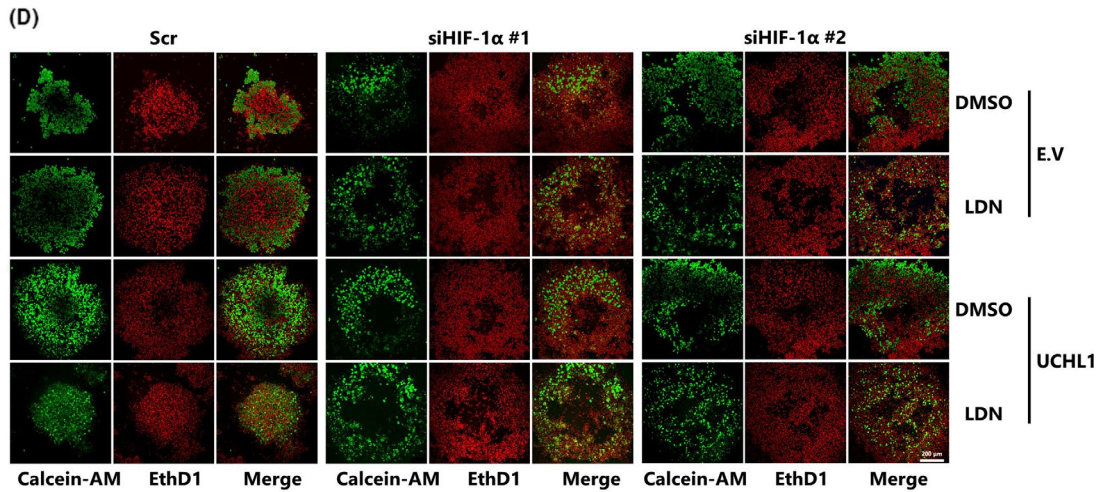
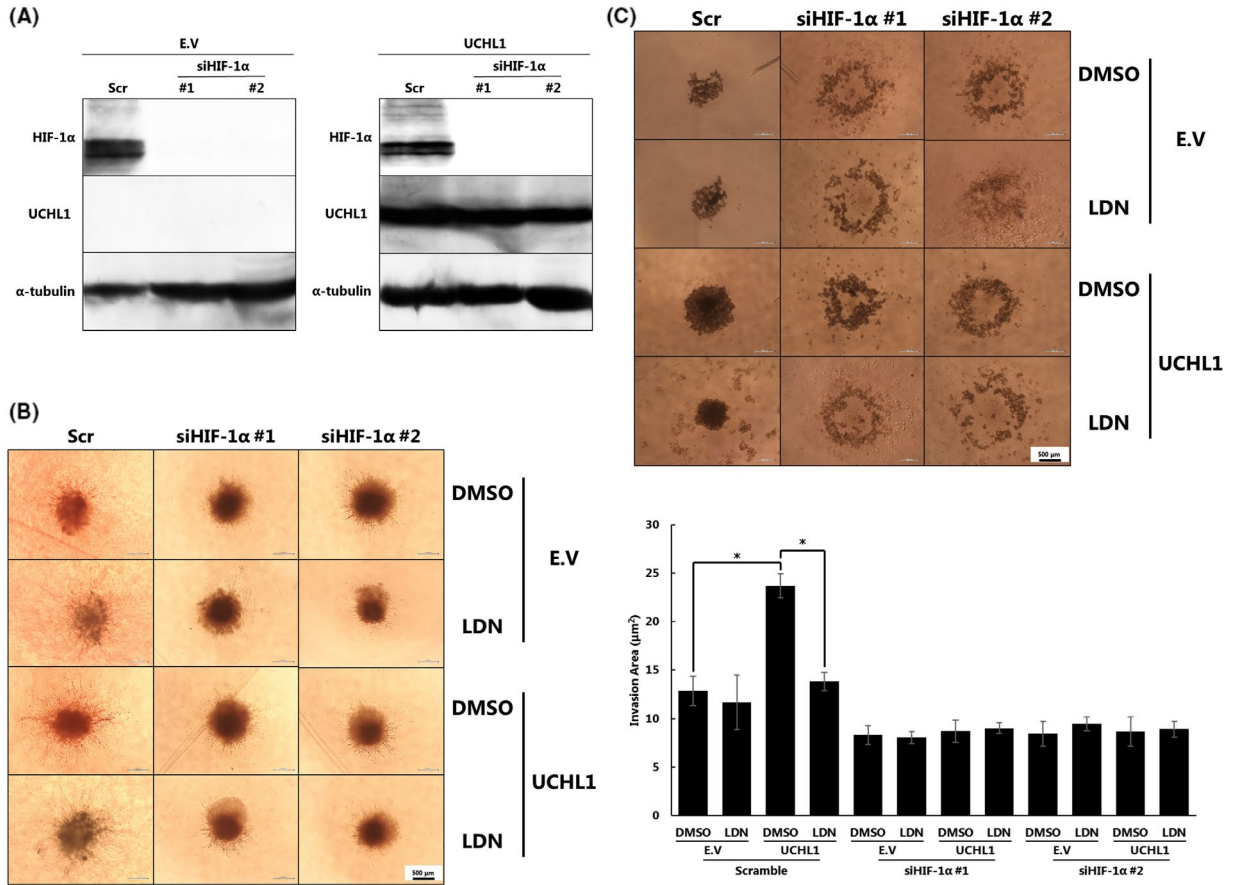
As HIF-1 $\alpha$  is a critical factor in transactivation modulation, we conducted 5HRE-luciferase (5HRE-Luc) gene reporter assays in which HeLa cells were stably transfected with the firefly luciferase gene driven by 5HRE to measure HIF activity. The UCHL1-expressing group showed a significant increase in 5HRE-Luc activity under both normoxia and hypoxia (Figure 2A). To investigate whether the UCHL1 inhibitor could affect HIF-1 activity, we further stably transfected HeLa/5HRE-Luc cells with UCHL1 expressing vector and treated these cells with various concentrations of LDN57444. This resulted in a significant decrease in the reporter activity in a dose-dependent manner (IC<sub>50</sub>: 3.7  $\mu$ mol/L; Figure 2B). Using the same cells, we also found that treatment of LDN57444 decreased the accumulation of 5HRE-luciferase protein expression compared with the DMSO-treated group under hypoxia. Camptothecin, a type I topoisomerase inhibitor that blocks global transcription activation was used as a positive control (Figure 2C). We then performed ODD-luciferase (ODD-Luc) assays to further determine the effect of UCHL1 on HIF-1 $\alpha$  stability. HeLa cells were stably transfected with a gene encoding luciferase N-terminally fused with the ODD domain of HIF-1 $\alpha$ , which was driven by the SV40 promoter. Under normoxia, the ODD domain is hydroxylated and subsequently ubiquitinated by pVHL to be rapidly degraded with a fused luciferase protein. However, under hypoxia, because of the insufficient oxygen for hydroxylation, the ODD-luciferase protein escapes from ubiquitination to release luminescence. Thus, this ODD-luciferase assay exactly mimics the process by which HIF-1 $\alpha$  is accumulated or degraded but in a highly

quantitative manner. We found that under both normoxia and hypoxia, the overexpression of UCHL1 led to a significant increase in the ODD-Luc activity while LDN57444 eliminated this effect (Figure 2D and S2). When confirming by immunostaining analysis, the protein expression of HIF-1 $\alpha$  was significantly elevated in UCHL1-transfected cells, while treatment with LDN57444 abrogated this increase in both nucleus and cytosol (Figure 2E,F and S1). To identify whether inhibition of UCHL1 could deactivate the downstream activity of the UCHL1-HIF-1 $\alpha$  axis, we analyzed the effect of LDN57444 on the expression of two typical cancer-related HIF-1 $\alpha$  target genes, *GLUT1* and *CA9*, in both MDA-MB-231 and MDA-MB-436 cells. In UCHL1-non-expressing MDA-MB-231 cells, blockade of UCHL1 by LDN57444 had no significant influence on the expression of both genes. In UCHL1-expressing MDA-MB-436 cells, however, LDN57444 lowered the expression of both genes remarkably under normoxia, while this effect was further amplified under hypoxia, revealing the specificity of the UCHL1 inhibitor (Figure 2G,H). In conclusion, UCHL1 increased the stability of HIF-1 $\alpha$  protein to promote HIF-1 activity while UCHL1 inhibition could eliminate this effect.

In murine models of pulmonary metastasis, UCHL1 has previously been shown to have an important role in the promotion of tumor cell metastasis.<sup>27</sup> To evaluate whether UCHL1 inhibitor has an anti-metastasis effect, we performed wound healing and transwell migration assays in cultured cells. Treatment with LDN57444 significantly suppressed the recovery of the scratched gap in MDA-MB-436 cells (76% inhibition), but not in MDA-MB-231 cells (Figure 2I,J). In the transwell migration assay, a similar result was obtained. LDN57444 treatment led to a striking decrease in the number of migrated MDA-MB 436 cells. Meanwhile, in MDA-MB-231 cells, no such effect was confirmed (Figure 2K,L). Finally, we examined whether this difference was possibly induced by a potential inhibitory effect of LDN57444 on the proliferation of MDA-MB-436 cells. We treated both MDA-MB-231 and MDA-MB-436 cells with 2.5  $\mu$ mol/L of LDN57444 and found no difference in cell number between both cell lines after 8, 24 and 48 hours (Figure 2M). Overall, UCHL1 inhibition showed efficacy against UCHL1-mediated cell migration in endogenous UCHL1-expressing cells.

### 3.3 | Ubiquitin carboxyl-terminal hydrolase L1 deficiency or inhibition leads to ubiquitin carboxyl-terminal hydrolase L1-dependent cell death in 3D culture

It has been demonstrated in many studies that anchorage-independent cultured cells can form spheroids.<sup>28</sup> Spheroids usually contain three areas: the proliferative area in the outer layer, the



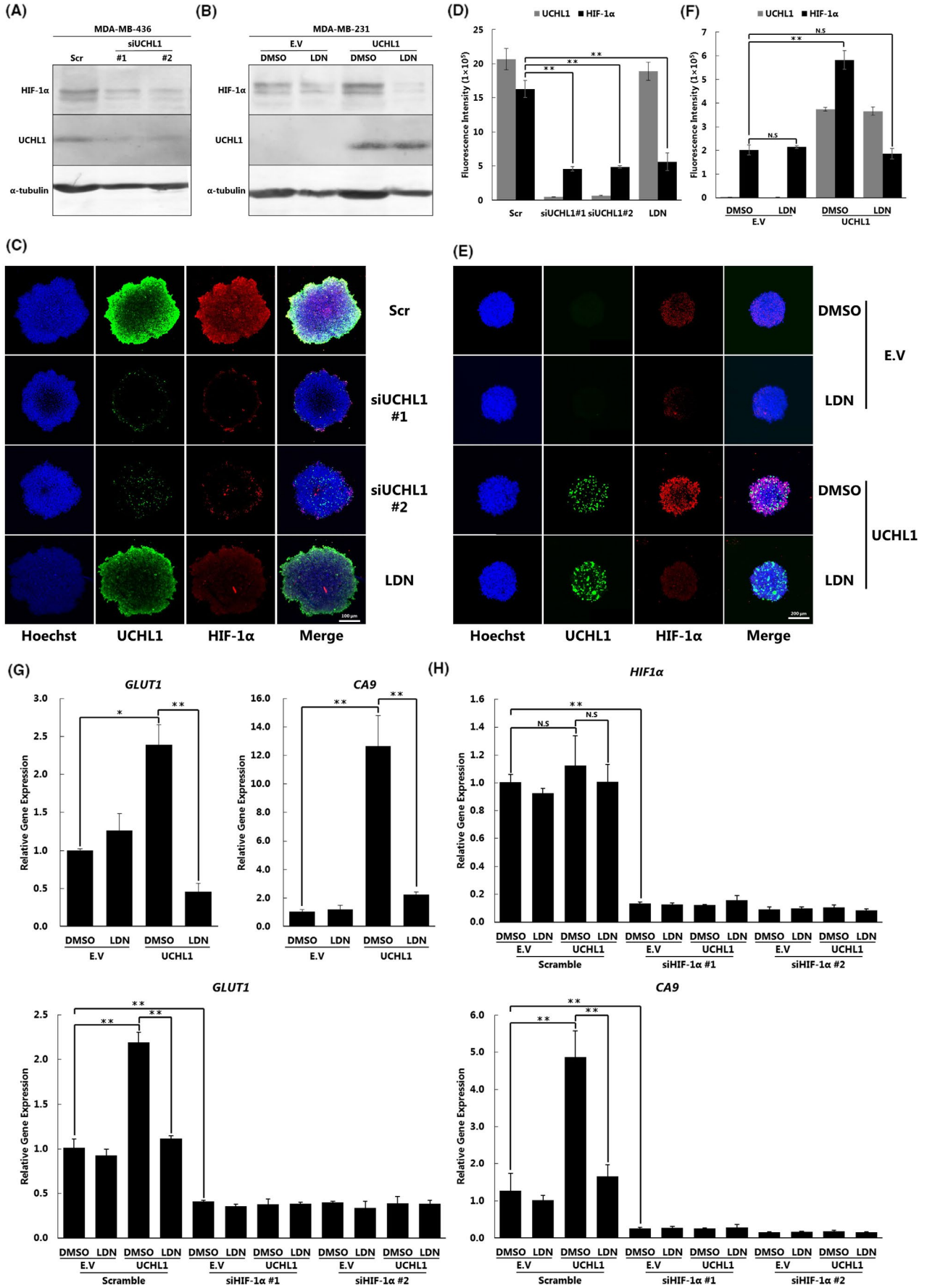


**FIGURE 5** Ubiquitin carboxyl-terminal hydrolase L1 (UCHL1) inhibition reduces hypoxia-inducible factor 1 $\alpha$  (HIF-1 $\alpha$ ) protein expression under 3D culture. A, *UCHL1*-depleted or mock-transfected MDA-MB-436 cells were seeded on ULA spheroid microplates for 5 d before western blotting analysis. B, *UCHL1*-transfected or mock-transfected MDA-MB-231 cells were seeded on ULA spheroid microplates for 5 d, treated with DMSO or LDN57444 (15  $\mu$ mol/L) for 48 h and subjected to western blotting analysis. C, Scr or si*UCHL1*-transfected or LDN57444 (15  $\mu$ mol/L)-treated MDA-MB-436 cells were seeded on ULA spheroid microplates for 5 d for 3D immunostaining. D, Quantification of results of C. E, *UCHL1*-transfected or mock-transfected MDA-MB-231 cells were seeded on ULA spheroid microplates for 5 d, treated with DMSO or LDN57444 (15  $\mu$ mol/L) for 48 h, and subjected to 3D immunostaining with the indicated antibodies. F, Quantification of results of E. G, H, *UCHL1*-transfected or mock-transfected (G) or empty vector (EV)/*UCHL1* and Scr/siHIF-1 $\alpha$ -co-transfected (H) MDA-MB-231 cells were seeded on ULA spheroid microplates for 5 d, treated with DMSO or LDN57444 (15  $\mu$ mol/L) for 48 h, and subjected to RT-qPCR to quantify the mRNA levels of the indicated genes. Data is shown as mean  $\pm$  SD;  $n = 3$ . Error bar indicates SD of the mean of three independent tests. \* $P < 0.05$ , \*\* $P < 0.01$  was verified with Tukey's honestly significant difference test or Student's  $t$ -test

quiescent area in the intermediate layer and the necrotic core area in the central layer. Compared with traditional 2D monolayer cultures, spheroids share more similarities with solid tumor tissues in features such as lower pH, cell-cell interactions, interstitial pressure, and drug accessibility, as well as variations in O<sub>2</sub> and nutrient accessibility.<sup>28,31</sup> Among these, the specific property that makes them good models in the study of HIF-related malignancies is that they exhibit areas of varied oxygen conditions. Therefore, we performed 3D spheroid cell culture to learn more about the link between *UCHL1* and HIF-1-dependent tumor malignancy.

We first compared typical malignancy-related factors, such as equivalent diameter, spheroid area, volume, solidity, sphericity and viable cell number when cells were incubated in an anchorage-independent condition.<sup>32</sup> In *UCHL1*-transfected MDA-MB-231 cells, all factors were evidently elevated (Figure 3A,B). However, these factors were drastically reduced in si*UCHL1*-transfected MDA-MB-436 cells. In the case of *UCHL1* inhibitor treatment in MDA-MB-436 cells, LDN57444 abated the diameter, area, volume and viable cell number but had no significant effect on solidity and sphericity (Figure 3B).

The central part of a spheroid, which is named the necrotic area, has been reported to have a relatively lower cell viability. Thus, we first determined whether *UCHL1* transfection could rescue these centrally located cells. Living and dead cells were stained with Calcein-AM and EthD1, respectively. Surprisingly, transfection of *UCHL1* in MDA-MB-231 cells was confirmed to rescue cells not only in the central but also in the intermediate layer of the quiescent area. Moreover, more living cells were confirmed in the proliferative area of *UCHL1*-transfected cells, suggesting a proliferation-promoting effect of *UCHL1* under 3D culture conditions (Figure 3C and S3). When MDA-MB-436 cells were treated with LDN57444 or transfected with siRNA against *UCHL1*, global cell death was dramatically increased compared with the control group. Therefore, we consider that the rescue of cell death and the increase in proliferation both contributed to the increase in total viable cell number (Figure 3C).

In 3D cultured models, metastasis in breast cancer cell is promoted due to features such as low oxygen, low pH and low glucose environments.<sup>33</sup> Therefore, we applied a 3D cell invasion assay to confirm whether *UCHL1* could have a metastasis-promoting effect in spheroid models. Transfection of *UCHL1* substantially promoted cell invasion under 3D culture conditions, while treatment with LDN57444 eliminated this increase (Figure 3D). In conclusion,

*UCHL1* increases malignant potential in spheroid cultured tumor cells, while its deficiency or inhibition can abrogate this effect.

### 3.4 | Ubiquitin carboxyl-terminal hydrolase L1 inhibition decreases viable cell number and invasiveness under 3D culture in a hypoxia-inducible factor 1 $\alpha$ -dependent manner

To examine whether the phenotypes observed in Figure 3 were induced in an HIF-1 $\alpha$ -dependent manner, we performed a co-transfection of *UCHL1* and siHIF-1 $\alpha$  in MDA-MB-231 cells (Figure 4A). We first examined whether the overexpression of *UCHL1* in HIF-1 $\alpha$  deficient cells could still affect spheroid phenotypes due to its deubiquitinating activity against other potential substrates except for HIF-1 $\alpha$ . We found that neither the transfection of *UCHL1* nor the treatment of LDN57444 showed any effect on the invasiveness in the siHIF-1 $\alpha$  transfected groups (Figure 4B). We further examined other malignancy-related factors and found that the siHIF-1 $\alpha$ -transfected spheroids were hollowed in the central part of the sphere, despite *UCHL1*-transfection, LDN57444-treatment or their combination (Figure 4C). Because HIF-1 $\alpha$  is mostly accumulated in the necrotic and quiescent layers of spheroids and is indispensable for their viability,<sup>29</sup> depletion of HIF-1 $\alpha$  almost completely disassembled the spheroid. When quantified (Figure S4), siHIF-1 $\alpha$  groups in general showed a drastically lower solidity, sphericity, volume and cell number compared with the scrambled-transfected group. When HIF-1 $\alpha$  deficient cells were transfected with *UCHL1* or further treated with LDN57444, no variation was found in these malignancy-related factors.

Finally, spheroid cells showed no difference in the number of live or dead between the empty vector (EV)-transfected and *UCHL1*-transfected groups (Figure 4D) in siHIF-1 $\alpha$ -transfected groups. These results demonstrate the dependency on HIF-1 $\alpha$  for *UCHL1* to raise tumor cell malignancy, while the blockade of the *UCHL1*-HIF-1 $\alpha$  axis abrogated this effect.

### 3.5 | Ubiquitin carboxyl-terminal hydrolase L1 inhibition reduces hypoxia-inducible factor 1 $\alpha$ protein expression under 3D culture

To confirm whether the observed malignancy-promoting effect could be ascribed to the activation of the *UCHL1*-HIF-1 $\alpha$  axis, we

investigated HIF-1 $\alpha$  protein levels in scrambled-transfected or siUCLH1-transfected cells under 3D culture. We found that the absence of UCLH1 clearly decreased HIF-1 $\alpha$  accumulation (Figure 5A). In MDA-MB-231 cells, as confirmed in 2D culture, overexpression of UCLH1 increased the protein expression of HIF-1 $\alpha$ , while LDN57444 treatment eliminated this effect (Figure 5B). Immunostaining of 3D cultures verified that silencing of the *UCLH1* gene had a similar effect compared with that of LDN57444, which significantly suppressed the protein expression of HIF-1 $\alpha$  (Figure 5C,D). In addition, MDA-MB-231 cells with UCLH1 overexpression showed higher HIF-1 $\alpha$  expression in all central, quiescent and proliferative areas. LDN57444 treatment once again remarkably decreased this effect (Figure 5E,F). The expression of two typical HIF-1 $\alpha$  downstream genes, *GLUT1* and *CA9*, was also elevated by UCLH1 overexpression in MDA-MB-231 cells, while this effect was abrogated by LDN57444 (Figure 5G). Finally, UCLH1 failed to increase the expression of both genes in siHIF-1 $\alpha$ -transfected groups (Figure 5H). Considering that *GLUT1* and *CA9* are both essential in tumor malignancy, we suppose this HIF-1 $\alpha$ -dependent upregulation on both genes by UCLH1 is a critical cause of the phenotypes observed in Figure 4. In conclusion, UCLH1 was confirmed to increase cell viability and proliferation as well as metastasis potential by stabilizing HIF-1 $\alpha$  to increase HIF-1 activity in the spheroid 3D culture system.

## 4 | DISCUSSION

In the present study, we investigated the impact of pharmacological inhibition of the deubiquitinating activity of UCLH1 on HIF-1-dependent tumor malignancy in a 3D cell culture system. We clearly showed that LDN57444 (Figure S5), a well-known UCLH1 inhibitor, attenuated HIF-1 $\alpha$  protein accumulation and lowered mRNA expression levels, causing cell death and reduced cell invasiveness in MDA-MB-436 as well as UCLH1-transfected MDA-MB-231 spheroids in an HIF-1 $\alpha$ -dependent manner. These results indicated that therapeutic strategies targeting UCLH1 are plausible for HIF-1 $\alpha$ -dependent tumors.

As shown in Figure 2, LDN57444 more effectively suppressed hypoxia-induced expression of *GLUT1* and *CA9* in MDA-MB-436 cells cultured under hypoxic conditions than normoxia cultured cells. It has been reported that in Hep3B cells cultured in hypoxic conditions, HIF-1 $\alpha$  is ubiquitinated and the blockade of Ub-activating enzyme (E1 enzyme) by a specific inhibitor, UBE1-41, resulted in an accumulation of HIF-1 $\alpha$  protein. These findings indicate that HIF-1 $\alpha$  is also degraded via the Ub-proteasome pathway under hypoxia.<sup>34</sup> While the pVHL E3 ligase-dependent degradation pathway is recognized as a dominant regulator of HIF-1 $\alpha$  under normoxia, hypoxia-associated factor,<sup>35</sup> receptor of activated protein kinase C 1 (RACK1)<sup>36</sup> and parkin<sup>37</sup> were identified as E3 ligases catalyzing the oxygen-independent ubiquitination of HIF-1 $\alpha$ . UCLH1 contributes to the escape of a variety of proteins from their turnover in a hydrolase activity-dependent manner, including HIF-1 $\alpha$ , by forming a UCLH1-HIF-1 $\alpha$  complex,

which is more abundantly detected in the nuclei of hypoxia-exposed HeLa cells.<sup>27</sup> Given that UCLH1 disassembles Lys48-linked poly-Ub chains conjugated to  $\beta$ -catenin5, epidermal growth factor receptor<sup>38</sup> and NOXA,<sup>39</sup> it is possible that UCLH1 stabilizes HIF-1 $\alpha$  protein levels in hypoxic conditions through the removal of poly-Ub chains attached via an oxygen-independent mechanism or interference with Ub modification of HIF-1 $\alpha$  by E3 ligases such as parkin. Furthermore, in Figure 5G, gene expression of *GLUT1* and *CA9* were both downregulated in spheroids to a much greater degree. Because spheroids have a mixture of oxygen conditions, it is plausible that LDN57444 showed a much severer impact on HIF-1-dependent tumor malignancy in our 3D spheroid model. Therefore, blockade of the UCLH1-HIF-1 $\alpha$  axis through UCLH1 inhibition can be a promising therapeutic strategy for the treatment of HIF-1-dependent tumors.

Ubiquitin carboxyl-terminal hydrolase L1 has been shown to promote tumor metastasis and cell proliferation via multiple signal transduction pathways. One is the stimulation of AKT through the inhibition of PH domain and leucine rich repeat protein phosphatase (PHLPP1), a negative regulator of AKT.<sup>40</sup> Moreover, following the stabilization of both  $\beta$ -catenin (oxygen-independent) and HIF-1 (oxygen-independent), subsequent activation of c-Jun N-terminal kinase (JNK) and p38 mitogen-activated protein (MAP) kinases<sup>41</sup> promotes the expression of several genes controlling the metastasis, invasion and proliferation of cancer cells, such as matrix metalloproteinases (MMP), cyclin D1 and c-Myc.<sup>42</sup> Because overexpression of UCLH1 failed to increase the malignancy-related factors in HIF-1 $\alpha$  deficient spheroid cells, we consider that UCLH1-HIF-1 $\alpha$  axis is the dominant pathway rather than the other two in UCLH1-mediated tumors. In fact, as both AKT<sup>43</sup> and Wnt/ $\beta$ -catenin<sup>44</sup> signaling have been reported to have crosstalk with HIF-1 $\alpha$ , the central role of HIF-1 $\alpha$  in UCLH1-mediated tumor malignancy is further confirmed.

Although the vital catalytic role of UCLH1 in the metastasis and aggravation of malignant tumors was confirmed in our research, the development of efficient UCLH1 inhibitors is still required, as only LDN57444 has been reported thus far.<sup>45</sup> However, LDN57444 is not suitable for clinical application due to its side-effects, which include induction of endoplasmic reticulum stress and abnormal expression of synapse proteins.<sup>1,46,47</sup> Therefore, the development of more effective and selective UCLH1 inhibitors remains a major challenge for the treatment of malignant tumors. The experiments we applied herein can be considered as an approach for the screening of potent UCLH1 inhibitors. In particular, the 3D spheroid system using UCLH1-expressing tumor cells provides valuable information for the validation of UCLH1 inhibitor screening. We are now applying our in-house chemical library, which includes synthetic molecules as well as natural products, to identify novel UCLH1 inhibitors.

## ACKNOWLEDGMENTS

This work was supported in part by a Grant-in-Aid for Scientific Research on Innovative Areas "Frontier Research on Chemical Communications" (No. 17H06401 to HK), a Grant-in-Aid for Scientific Research (No. 19H02840 to HK) from the Ministry of

Education, Culture, Sports, Science and Technology (MEXT), Japan, the Project for Development of Innovative Research on Cancer Therapeutics (P-DIRECT) (No. 15cm0106117h0002 to HK) and the Platform Project for Supporting Drug Discovery and Life Science Research (No. JP19am0101092 to HK) from the Japan Agency for Medical Research and Development (AMED), Japan.

## CONFLICTS OF INTEREST

The authors have no conflicts of interest.

## ORCID

Hiroshi Harada  <https://orcid.org/0000-0001-7507-3173>

Hideaki Kakeya  <https://orcid.org/0000-0002-4293-7331>

## REFERENCES

- Davies CW, Chaney J, Korbel G, et al. The co-crystal structure of ubiquitin carboxy-terminal hydrolase L1 (UCHL1) with a tripeptide fluoromethyl ketone (Z-VAE (OMe)-FMK). *Bioorg Med Chem Lett*. 2012;22:3900-3904.
- Mtango NR, Sutovsky M, Susor A, Zhong Z, Latham KE, Sutovsky P. Essential role of maternal UCHL1 and UCHL3 in fertilization and preimplantation embryo development. *J Cell Physiol*. 2012;227:1592-1603.
- Wilkinson KD, Lee K, Deshpande S, Duerksen-Hughes P, Boss JM, Pohl J. The neuron-specific protein PGP 9.5 is a ubiquitin carboxyl-terminal hydrolase. *Science*. 1989;246:670-673.
- Latres E, Chiaur D, Pagano M. The human F box protein  $\beta$ -Trcp associates with the Cul1/Skp1 complex and regulates the stability of  $\beta$ -catenin. *Oncogene*. 1999;18:849.
- Zhong J, Zhao M, Ma Y, et al. UCHL1 acts as a colorectal cancer oncogene via activation of the  $\beta$ -catenin/TCF pathway through its deubiquitinating activity. *Int J Mol Med*. 2012;30:430-436.
- Liu Y, Fallon L, Lashuel HA, Liu Z, Lansbury PT Jr. The UCH-L1 gene encodes two opposing enzymatic activities that affect  $\alpha$ -synuclein degradation and Parkinson's disease susceptibility. *Cell*. 2002;111:209-218.
- Jackson P, Thompson R. The demonstration of new human brain-specific proteins by high-resolution two-dimensional polyacrylamide gel electrophoresis. *J Neurol Sci*. 1981;49:429-438.
- Day IN, Thompson RJ. UCHL1 (PGP 9.5): neuronal biomarker and ubiquitin system protein. *Prog Neurobiol*. 2010;90:327-362.
- Chu K, Li H, Wada K, Johnson J. Ubiquitin C-terminal hydrolase L1 is required for pancreatic beta cell survival and function in lipotoxic conditions. *Diabetologia*. 2012;55:128-140.
- Honaramooz A, Megee SO, Rathi R, Dobrinski I. Building a testis: formation of functional testis tissue after transplantation of isolated porcine (*Sus scrofa*) testis cells. *Biol Reprod*. 2007;76:43-47.
- Pan X-Q, Gonzalez JA, Chang S, Chacko S, Wein AJ, Malykhina AP. Experimental colitis triggers the release of substance P and calcitonin gene-related peptide in the urinary bladder via TRPV1 signaling pathways. *Exp Neurol*. 2010;225:262-273.
- Seliger B, Handke D, Schabel E, Bukur J, Lichtenfels R, Dammann R. Epigenetic control of the ubiquitin carboxyl terminal hydrolase 1 in renal cell carcinoma. *J Transl Med*. 2009;7:90.
- Sasaki H, Yukiue H, Moriyama S, et al. Expression of the protein gene product 9.5, PGP9.5, is correlated with T-status in non-small cell lung cancer. *Jpn J Clin Oncol*. 2001;31:532-535.
- Gu Y-Y, Yang M, Zhao M, et al. The de-ubiquitinase UCHL1 promotes gastric cancer metastasis via the Akt and Erk1/2 pathways. *Tumor Biol*. 2015;36:8379-8387.
- Bheda A, Yue W, Gullapalli A, et al. Positive reciprocal regulation of ubiquitin C-terminal hydrolase L1 and  $\beta$ -catenin/TCF signaling. *PLoS ONE*. 2009;4:e5955.
- Jensen RL, Ragel BT, Whang K, Gillespie D. Inhibition of hypoxia inducible factor-1 $\alpha$  (HIF-1 $\alpha$ ) decreases vascular endothelial growth factor (VEGF) secretion and tumor growth in malignant gliomas. *J Neurooncol*. 2006;78:233-247.
- Takeya H. Natural products-prompted chemical biology: phenotypic screening and a new platform for target identification. *Nat Prod Rep*. 2016;33:648-654.
- Yoshimura A, Nishimura S, Otsuka S, Hattori A, Takeya H. Structure elucidation of verucopeptin, a HIF-1 inhibitory polyketide-hexapeptide hybrid metabolite from an Actinomycete. *Org Lett*. 2015;17:5364-5367.
- Yasuda Y, Arakawa T, Nawata Y, et al. Design, synthesis, and structure-activity relationships of 1-ethylpyrazole-3-carboxamide compounds as novel hypoxia-inducible factor (HIF)-1 inhibitors. *Bioorg Med Chem*. 2015;23:1776-1787.
- Kaelin WG Jr, Ratcliffe PJ. Oxygen sensing by metazoans: the central role of the HIF hydroxylase pathway. *Mol Cell*. 2008;30:393-402.
- Bertout JA, Patel SA, Simon MC. The impact of O<sub>2</sub> availability on human cancer. *Nat Rev Cancer*. 2008;8:967.
- Salceda S, Caro J. Hypoxia-inducible factor 1 $\alpha$  (HIF-1 $\alpha$ ) protein is rapidly degraded by the ubiquitin-proteasome system under normoxic conditions Its stabilization by hypoxia depends on redox-induced changes. *J Biol Chem*. 1997;272:22642-22647.
- Marxsen J, Stengel P, Doege K, et al. Hypoxia-inducible factor-1 (HIF-1) promotes its degradation by induction of HIF- $\alpha$ -prolyl-4-hydroxylases. *Biochem J*. 2004;381:761-767.
- Hon W-C, Wilson MI, Harlos K, et al. Structural basis for the recognition of hydroxyproline in HIF-1 $\alpha$  by pVHL. *Nature*. 2002;417:975.
- Reyes H, Reisz-Porszasz S, Hankinson O. Identification of the Ah receptor nuclear translocator protein (Arnt) as a component of the DNA binding form of the Ah receptor. *Science*. 1992;256:1193-1195.
- Stolze IP, Tian Y-M, Appelhoff RJ, et al. Genetic analysis of the role of the asparaginyl hydroxylase factor inhibiting hypoxia-inducible factor (HIF) in regulating HIF transcriptional target genes. *J Biol Chem*. 2004;279:42719-42725.
- Goto Y, Zeng L, Yeom CJ, et al. UCHL1 provides diagnostic and antimetastatic strategies due to its deubiquitinating effect on HIF-1 $\alpha$ . *Nat Commun*. 2015;6:6153.
- Edmondson R, Broglie JJ, Adcock AF, Yang L. Three-dimensional cell culture systems and their applications in drug discovery and cell-based biosensors. *Assay Drug Dev Technol*. 2014;12:207-218.
- Bhang SH, Cho S-W, La W-G, et al. Angiogenesis in ischemic tissue produced by spheroid grafting of human adipose-derived stromal cells. *Biomaterials*. 2011;32:2734-2747.
- Schneider CA, Rasband WS, Eliceiri KW. NIH Image to ImageJ: 25 years of image analysis. *Nat Methods*. 2012;9:671.
- Antoni D, Burckel H, Josset E, Noel G. Three-dimensional cell culture: a breakthrough in vivo. *Int J Mol Sci*. 2015;16:5517-5527.
- Zanoni M, Piccinini F, Arienti C, et al. 3D tumor spheroid models for in vitro therapeutic screening: a systematic approach to enhance the biological relevance of data obtained. *Sci Rep*. 2016;6:19103.
- Benton G, DeGray G, Kleinman HK, George J, Arnaoutova I. In vitro microtumors provide a physiologically predictive tool for breast cancer therapeutic screening. *PLoS ONE*. 2015;10:e0123312.
- Wang R, Zhang P, Li J, Guan H, Shi G. Ubiquitination is absolutely required for the degradation of hypoxia-inducible factor-1 alpha protein in hypoxic conditions. *Biochem Biophys Res Commun*. 2016;470:117-122.
- Koh MY, Powis G. HIF: the new player in oxygen-independent HIF-1 $\alpha$  degradation. *Cell Cycle*. 2009;8:1359-1366.
- Liu YV, Baek JH, Zhang H, Diez R, Cole RN, Semenza GL. RACK1 competes with HSP90 for binding to HIF-1 $\alpha$  and is required for

- O<sub>2</sub>-independent and HSP90 inhibitor-induced degradation of HIF-1 $\alpha$ . *Mol Cell*. 2007;25:207-217.
37. Liu J, Zhang C, Zhao Y, et al. Parkin targets HIF-1 $\alpha$  for ubiquitination and degradation to inhibit breast tumor progression. *Nat Commun*. 2017;8:1823.
  38. Jin Y, Zhang W, Xu J, et al. UCH-L1 involved in regulating the degradation of EGFR and promoting malignant properties in drug-resistant breast cancer. *Int J Clin Exp Pathol*. 2015;8:12500.
  39. Brinkmann K, Zigrino P, Witt A, et al. Ubiquitin C-terminal hydrolase-L1 potentiates cancer chemosensitivity by stabilizing NOXA. *Cell Rep*. 2013;3:881-891.
  40. Zhou C, Huang C, Wang J, et al. LncRNA MEG3 downregulation mediated by DNMT3b contributes to nickel malignant transformation of human bronchial epithelial cells via modulating PHLPP1 transcription and HIF-1 $\alpha$  translation. *Oncogene*. 2017;36:3878.
  41. Tacchini L, Dansi P, Matteucci E, Desiderio MA. Hepatocyte growth factor signalling stimulates hypoxia inducible factor-1 (HIF-1) activity in HepG2 hepatoma cells. *Carcinogenesis*. 2001;22:1363-1371.
  42. Li Y-J, Wei Z-M, Meng Y-X, Ji X-R.  $\beta$ -catenin up-regulates the expression of cyclinD1, c-myc and MMP-7 in human pancreatic cancer: Relationships with carcinogenesis and metastasis. *World J Gastroenterol*. 2005;11:2117.
  43. Zhang BO, Li Y-L, Zhao J-L, et al. Hypoxia-inducible factor-1 promotes cancer progression through activating AKT/Cyclin D1 signaling pathway in osteosarcoma. *Biomed Pharmacother*. 2018;105:1-9.
  44. Kaidi A, Williams AC, Paraskeva C. Interaction between  $\beta$ -catenin and HIF-1 promotes cellular adaptation to hypoxia. *Nat Cell Biol*. 2007;9:210.
  45. Liu Y, Lashuel HA, Choi S, et al. Discovery of inhibitors that elucidate the role of UCH-L1 activity in the H1299 lung cancer cell line. *Chem Biol*. 2003;10:837-846.
  46. Tan Y-Y, Zhou H-Y, Wang Z-Q, Chen S-D. Endoplasmic reticulum stress contributes to the cell death induced by UCH-L1 inhibitor. *Mol Cell Biochem*. 2008;318:109-115.
  47. Gong B, Cao Z, Zheng P, et al. Ubiquitin hydrolase Uch-L1 rescues  $\beta$ -amyloid-induced decreases in synaptic function and contextual memory. *Cell*. 2006;126:775-788.

#### SUPPORTING INFORMATION

Additional supporting information may be found online in the Supporting Information section.

**How to cite this article:** Li X, Hattori A, Takahashi S, Goto Y, Harada H, Kakeya H. Ubiquitin carboxyl-terminal hydrolase L1 promotes hypoxia-inducible factor 1-dependent tumor cell malignancy in spheroid models. *Cancer Sci*. 2020;111:239-252. <https://doi.org/10.1111/cas.14236>